Letter

Design of Thermoresponsive Polyamine Cross-Linked Perfluoropolyether Hydrogels for Imaging and Delivery Applications

Michele Herneisey,[∥] Paula Flórez Salcedo,[∥] Trystan Domenech, Christina Bagia, Simon S. George, Robert Tunney, Sachin Velankar, T. Kevin Hitchens, and Jelena M. Janjic*
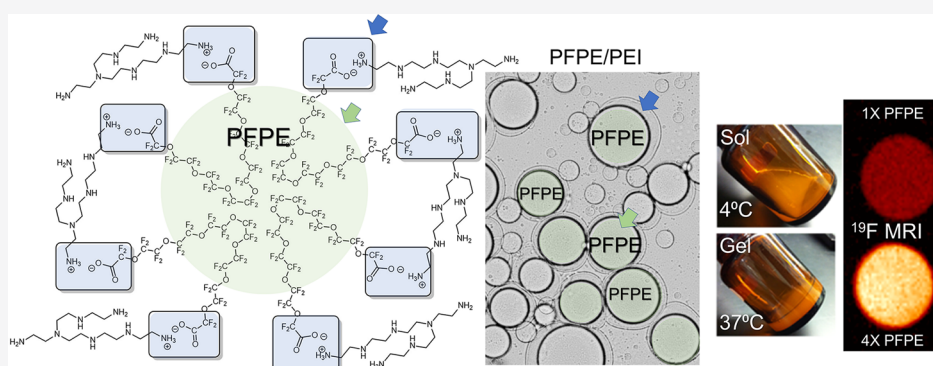
Read Online

ACCESS | Metrics & More | Article Recommendations | Supporting Information

ABSTRACT: Perfluorocarbons are versatile compounds with applications in ^{19}F magnetic resonance imaging (MRI) and chemical conjugation to drugs and pH sensors. We present a novel thermoresponsive perfluorocarbon emulsion hydrogel that can be detected by ^{19}F MRI. The developed hydrogel contains perfluoro(polyethylene glycol dimethyl ether) (PFPE) emulsion droplets that are stabilized through ionic cross-linking with polyethylenimine (PEI). Specifically, PFPE ester undergoes hydrolysis upon contact with aqueous PEI solution, resulting in an ionic bond between the PFPE acid and charged PEI amino groups. Due to the ionic nature of the PFPE/PEI bond, potassium buffer is required to preserve the hydrogel's pH and rheological and emulsion droplet stability. The presence of the surface cross-linked PFPE droplets does not affect the hydrogel's rheological behavior, drug loading, or drug release, and the hydrogel is nontoxic. We propose that the presented hydrogel can be adapted to a broad range of biomedical imaging and delivery applications.

KEYWORDS: Hydrogel, perfluorocarbon, perfluoropolyether, polyethylenimine, ^{19}F magnetic resonance imaging

Though the development of pharmaceutical hydrogels continues to accelerate, these formulations often encounter substantial challenges during scale up and clinical translation. The application of simple, low-energy manufacturing approaches to the development of multifunctional hydrogel formulations may help to ease this transition. In the presented work, an in situ low-energy approach was used to develop a versatile, thermoresponsive, cross-linked perfluorocarbon (PFC) emulsion hydrogel. Since their FDA-approval in 1989 as blood substitutes,[1] PFCs have gained increasing interest. PFCs are fluorinated hydrocarbons and, as such, can be imaged using ^{19}F magnetic resonance imaging (MRI). Organic fluorine is not present in the human body; thus, PFC-containing biomaterials can be used to provide background-free imaging.[2−4] Some PFCs, such as perfluoro(polyethylene glycol dimethyl ether) (PFPE), are particularly versatile because they can be directly conjugated to imaging agents (fluorescent dyes, positron emission tomography chelators, etc.), pH sensors, or therapeutic drugs. The high electronegativity present in the

C−F bonds facilitates direct conjugation of primary and secondary amines with PFPE ester end groups.[5−7] Janjic et al. have developed PFPE nanoemulsions containing Bodipy-PFPE,[6] Cy3-PFPE, and CypHer5-PFPE conjugates.[7] This direct conjugation is advantageous, as it prevents differential tissue distribution of the fluorescent dye and the magnetic resonance reporter.[6] Further, incorporation of pH sensitive conjugates (CypHer5-PFPE) into PFPE nanoemulsions has been used to track their specific intracellular location upon uptake.[7]

PFCs also have the ability to dissolve large volumes of respiratory gases and serve as oxygen carriers.[8] Providing
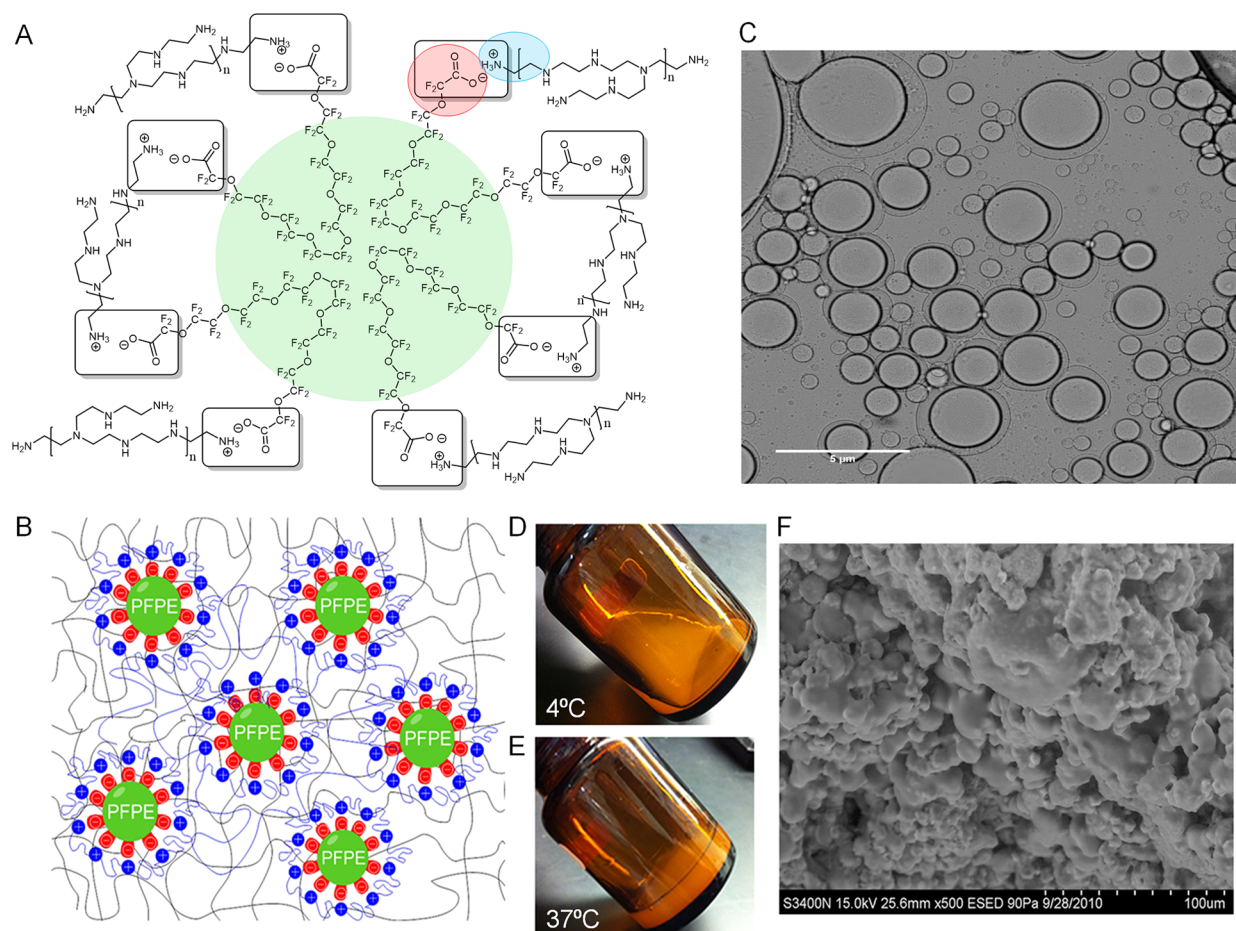
Figure 1. (A) Structural schematic of the ionic interaction of PFPE carboxyl ion end groups, which are released following PFPE-Ester hydrolysis in aqueous medium, and ionized quaternary groups on exposed chains of branched 25 kDa PEI, resulting in ammonium salt bridges responsible for droplet surface stabilization at the PFPE/water interface. (B) Schematic representation of PFPE ionic surface cross-linked interaction with PEI in F127 hydrogel matrix. (C) Cross polarized optical microscopy image of the surface interaction where PFPE droplets are surrounded by PEI in aqueous medium, 50× magnification. (D−E) PFPE/PEI/F127 hydrogel thermoresponsive behavior. Sol state at 4 °C and gel state at body temperature (37 °C). (F) Scanning electron microscopy image of lyophilized cross-linked PFPE/PEI/F127 hydrogel, showing large and small droplets of PFPE oil dispersed into F127 matrix.

sufficient delivery (drug, imaging agent, pH sensor, oxygen, etc.) over a period of several days or even weeks is a significant challenge associated with PFCs and other biomaterials. To address this limitation, we have developed a thermoresponsive, cross-linked PFC emulsion hydrogel. Hydrogels are generally defined as water-swollen, three-dimensional, hydrophilic polymer networks that can be cross-linked either physically or chemically.[9,10] Hydrogels are usually built with polymeric materials that offer a wide range of size, water content, and chemical properties (pH, charge, hydrogen donor/acceptor, cross-linking). Hydrogels also provide flexibility for new platforms in tissue engineering,[11] development of biomedical sensors,[12] design of novel drug delivery systems,[13] and contrast agents for imaging.[14] Oxygen delivery using PFC-containing hydrogels has been investigated as a potential therapy in wound healing and sciatic nerve regeneration. For example, Leipzig et al. have developed a fluorinated methacrylamide chitosan (MACF) hydrogel that was synthesized through PFC conjugation to chitosan free amines.[15−18] The developed MACF hydrogel was shown to improve regenerated wound tissue structure in a splinted transgenic diabetic mouse wound model.[18] Ma et al. have reported a perfluorotributylamine-based oxygen carrying fibrin hydrogel.[19] The developed

hydrogel was found to promote axonal regeneration and remyelination and accelerate motor and sensory function recovery of the sciatic nerve in rats. Alginate hydrogels containing perfluorooctyl bromide nanoemulsions have also been investigated for their potential applications as oxygen delivery platforms to 3-dimensional tissue-engineered constructs.[20,21]

Though PFC-containing hydrogels have a broad range of potential biomedical applications, the large-scale production of these biomaterials can be challenging. Since PFCs are both hydrophobic and lipophilic, PFC emulsions generally need to be produced using high energy methods prior to their incorporation into a hydrogel, such as sonication or microfluidization. In the presented work, the hydrogel formation process is streamlined to eliminate the high energy emulsification step. PFC emulsion droplets are formed via ionic interaction between PFPE and branched 25 kDa polyethylenimine (PEI). These PFPE-PEI emulsion droplets are stabilized in a thermoresponsive cross-linked Pluronic F127 (F127) hydrogel. The PFPE-PEI emulsion is formed synchronously within the F127 hydrogel using planetary mixing. This streamlined, low-energy process is amenable to
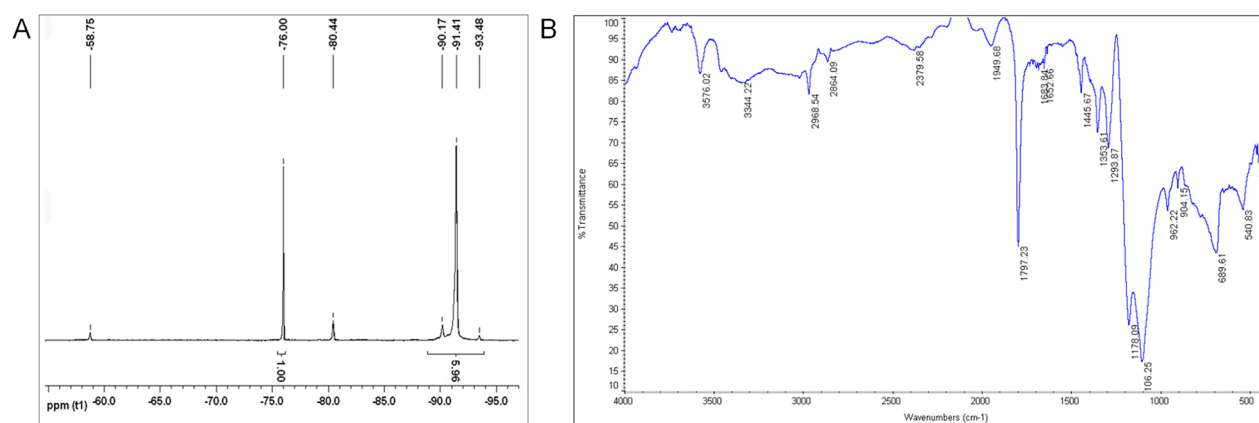
Figure 2. Spectroscopic characterization. (A) ^{19}F NMR spectrum of cross-linked PFPE/PEI/F127 hydrogel; (B) FT-IR spectrum of lyophilized cross-linked PFPE/PEI/F127 hydrogel.

future scale up using earlier established protocols with some modifications.[22]

The presented hydrogel is stable, nontoxic, and capable of being detected with ^{19}F MRI. This feature will allow for real-time, background-free visualization of hydrogel performance during its use as a drug and/or oxygen delivery platform. To demonstrate the hydrogel's potential as a drug delivery platform, the natural anti-inflammatory compound resveratrol was incorporated into the F127 micelles without altering hydrogel composition. Observed extended resveratrol release from the hydrogel suggests this technology could provide extended anti-inflammatory treatment through topical or transdermal delivery or through local implantation.

The versatility and novelty of the presented hydrogel comes from the integrated contribution of its three main components: (1) F127, (2) PFPE, and (3) PEI. F127 is a nontoxic, FDA-approved thermosensitive copolymer that undergoes gelation by heating above the lower critical gelation temperature (LCGT), meaning that its sol-to-gel transition occurs with an increase in temperature. LCGT hydrogels have gained attention in the biomedical field since they allow encapsulation under mild conditions and can undergo gelation when injected into the body.[23]

PEI is a cationic polymer commonly used in gene transfection.[24] Here, it is used to stabilize the PFPE droplets in the F127 hydrogel matrix. The presented data show that when incorporated into an aqueous based hydrogel matrix, PFPE ester undergoes immediate hydrolysis, creating a carboxylate ion that forms an ionic bond with the primary ammonium ions from basic branched PEI. Each PFPE methyl ester polymer has two ester end groups that hydrolyze to form a salt with quaternary ammonium salt groups formed at exposed primary amines on the branched 25 kDa PEI, forming a fluorocarbon rich insoluble network (Figure 1A). This ionic interaction creates a unique cross-linked network of PEI stabilized PFPE droplets in an aqueous F127 solution (Figure 1B). Incorporation of F127 causes the hydrogels to flow at 4 °C (Figure 1D) and gel at body temperature, 37 °C (Figure 1E). Rheological studies demonstrate that this thermoresponsive behavior is driven by the F127 matrix (Figures 3F−I and Figures S3−4, discussed further below).

The presence of primary amines on PEI and methyl ester end groups on PFPE can be utilized to functionalize this material with different imaging moieties, therapeutic small molecules, or biomolecules (e.g., proteins). For example, PEI has been used to coat a PFC nanoemulsion droplet and enable the addition of a breast cancer cell targeting antibody.[25] Therefore, we propose that in similar fashion, this strategy can be applied to functionalize dispersed PFPE droplets in the presented hydrogel.

We hypothesized that the PFPE−PEI interaction occurs at the fluorous/aqueous phase interface at the surface of PFPE droplets distributed in the hydrogel. To observe and analyze this surface reaction, PFPE and an aqueous PEI solution were gently mixed together and analyzed by optical microscopy with dual polarizing filters (Figure 1C). The microscopy revealed that the PFPE droplets are surrounded by a corona built primarily of PEI. This interaction forms a similar structure to the one found in biphasic emulsions with a lipophobic/hydrophobic PFPE droplet surrounded by a hydrophilic PEI coating.[6] Scanning electron microscopy was used to further confirm the PFPE−PEI hydrogel structure (Figure 1F). In the lyophilized sample, large PFPE oil droplets are dispersed throughout a matrix of F127 micelles.

To further characterize and investigate the nature of the surface interaction between PFPE and PEI, ^{19}F NMR and FT-IR were performed. The ^{19}F NMR chemical shift of the PFPE preterminal presented at −80.03 ppm, which matches earlier reported PFPE carboxylate end groups.[5] Previously, we reported that when PFPE reacts with a primary amine to form a PFPE amide, the chemical shift of the peak is shifted downfield due to the deshielding effect of the nitrogen atom, resulting in a peak between 74 and 78 ppm.[6] The ^{19}F NMR spectrum (Figure 2A) of the PFPE/PEI/F127 hydrogel shows the characteristic CF_2 present in all PFPE oils at −91.41 ppm[26] and a peak at −80.44 ppm, suggesting the presence of a carboxylate ammonium interaction between PFPE and PEI, where the slight chemical shift of 0.4 ppm is due to the deshielding effects of the nitrogen from the ammonium ion. The FT-IR spectrum (Figure 2B) shows a strong carbonyl peak at 1797 cm^{-1}. Carbonyl stretches associated with amide bonds are observed at lower wavenumbers between 1630 and 1660 cm^{-1}.[27] We suggest that the inductive effect of the carboxyl ion is increasing the force constant and frequency of absorption of the carbonyl, thus increasing the wavenumber and shifting the carbonyl peak. PFPE C−F stretches are clearly observed around 1110 cm^{-1}. The ammonium bands in the 2800−3600 cm^{-1} region are weak, making it difficult to distinguish whether the ammonium ions are secondary or tertiary. However, the nature of the PFPE/polymer interaction

Table 1. Composition of Hydrogels

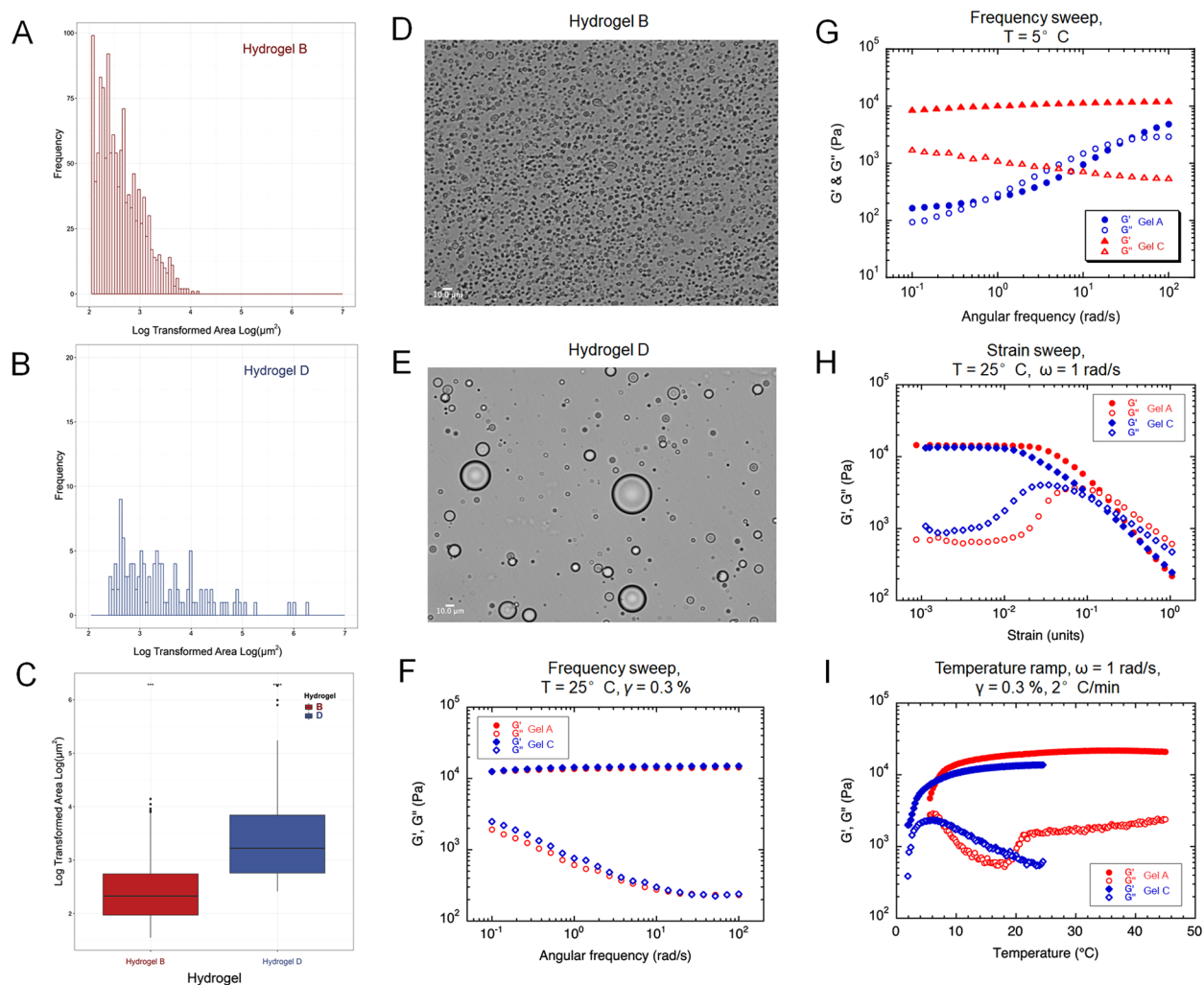| Hydrogels (25.75 mL)	Pluronic F127 (% w/v)	Glycerol (% w/v)	PEI (25 kDa) (% w/v)	PFPE Ester (% w/v)	PFPE Oxide (% w/v)	Buffer
A	21.00	24.47	0.07	12.24		No
B	21.00	24.47	0.07	12.24		Yes
C	21.00	24.47	0.07		12.24	No
D	21.00	24.47	0.07		12.24	Yes
E	21.00	24.47	0.07			No

Figure 3. Hydrogel characterization. (A−E) Histograms of droplet surface area distributions and images obtained by cross-polarized optical microscopy of hydrogel B (Panels A and D, cross-linked formulation with PFPE-Ester/PEI/F127) and hydrogel D (Panels B and E, non-cross-linked formulation with PFPE-Oxide/PEI/F127). Images obtained at 50× magnification. (C) Surface area distribution data for hydrogels B and D represented as a box plot. (F−I) Rheological behavior comparisons between PFPE-Ester (Hydrogel A) and PFPE-Oxide (Hydrogel C) hydrogels. Elastic modulus G' (filled symbols) and viscous modulus G'' (empty symbols) during oscillatory frequency at room temperature (Panel F) and 5 °C (Panel G). (H) Elastic modulus G' (filled symbols) and viscous modulus G'' (empty symbols) during sweeps and strain amplitude sweeps. (I) Strain sweep at increasing temperatures from 2 to 50 °C showing sol to gel transition comparable to pure F127 hydrogel.

at the surface is likely driving the surface reaction between highly acidic PFPE ester end groups and primary amines. The absence of the amide peak in the ^{19}F NMR and the shift of the carbonyl peak in the FT-IR spectra confirm that the cross-linked bond between PFPE and PEI is not covalent but ionic in nature and hence could be influenced by changes in the pH of the overall hydrogel.

To investigate the stability and rheological properties of the PFPE/PEI/F127 hydrogel, five hydrogels were manufactured (Table 1). PFPE carboxylate hydrolysis in water potentially drives the degradation of the dispersed PFPE droplets. To

investigate this possibility, PFPE-Ester/PEI/F127 hydrogels were developed with and without a pH 7.4 potassium buffer (Hydrogels A and B). PFPE-Oxide/PEI/F127 hydrogels were developed as controls because PFPE oxide lacks reactive end groups needed for PEI cross-linking (Hydrogels C and D). Additionally, a PFPE-free hydrogel with PEI (Hydrogel E) was developed as a control to evaluate the toxicity of the PFPE-Ester/PEI/F127 hydrogel *in vitro* (Figure 6, discussed further below).

Cross-polarized optical microscopy and rheology were used to further analyze the hydrogels' behavior and the effects of the
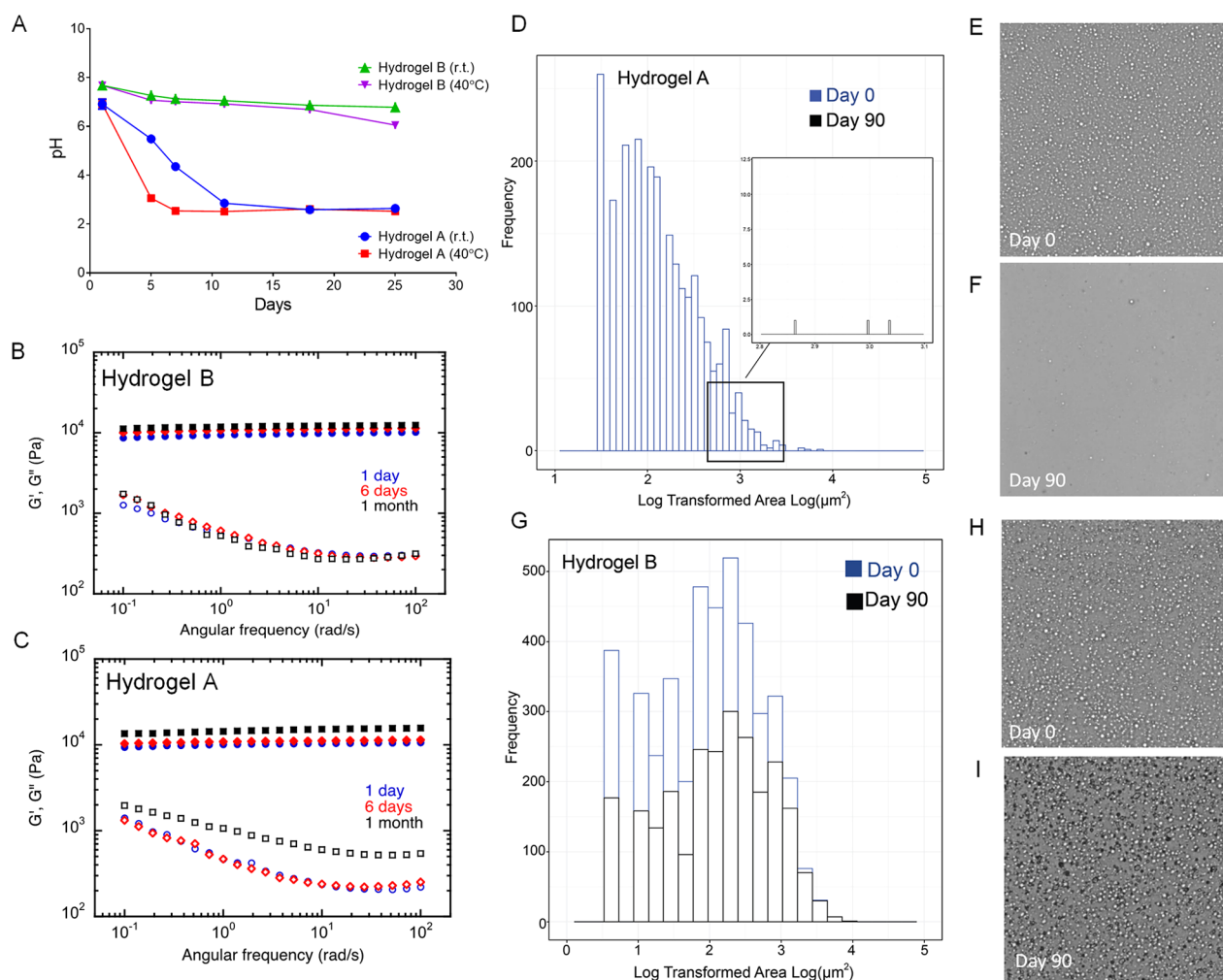
Figure 4. Impact of buffer on hydrogel stability. (A) pH measurements over time show a sharp drop in pH in nonbuffered cross-linked hydrogel (Hydrogel A) upon storage at room and elevated (40 °C) temperature. pH remains stable over time in the buffered cross-linked hydrogel (Hydrogel B). (B–C) Rheological behavior comparisons between buffered (Panel B) and nonbuffered (Panel C) PFPE/PEI/F127 cross-linked hydrogels. Elastic modulus G' (filled symbols) and viscous modulus G'' (empty symbols) during oscillatory frequency were measured at three different time-points (day 1, 6, and 30) upon storage at room temperature. Rheological change of the nonbuffered hydrogel indicates physicochemical degradation due to hydrolysis of the PFPE ester end groups. (D–G) Histograms of droplet surface area distributions obtained by cross-polarized optical microscopy of nonbuffered hydrogel A (Panel D) and buffered hydrogel B (Panel G). Microscopy images of hydrogel A (nonbuffered) at day 0 (Panel E) and after 90 days of storage at ambient temperature (Panel F); Microscopy images of hydrogel B (buffered) at day 0 (Panel H) and after 90 days of storage at ambient temperature (Panel I). Droplets degrade over time without the use of buffer, which corresponds to changes in pH (Panel A) and rheological behavior (Panel C).

PFPE–PEI surface interaction on the F127 matrix (Figure 3). Microscopy revealed significant differences in droplet surface area and distribution between hydrogels containing PFPE ester (Hydrogel B, Figure 3D) and PFPE oxide (Hydrogel D, Figure 3E). A new algorithm was developed and used to quantitatively measure these observable differences by measuring the surface area of each droplet distributed throughout the hydrogel matrix (Supporting Information Figure 1S). Log areas of the droplets' surface sizes were plotted as frequency histograms for hydrogel B (Figure 3A) and hydrogel D (Figure 3B). The data are also represented as a box plot (Figure 3C). The PFPE ester hydrogel has significantly smaller droplets than the PFPE oxide hydrogel, further confirming the presence of a PFPE-Ester/PEI ionic bond. This interaction results in charge-stabilized PFPE droplets that are evenly distributed throughout the hydrogel, which is a critical feature for any future delivery or imaging applications.

We also investigated the effects of gel composition on rheological behavior. Specifically, we investigated the impact of the cross-linking interactions between PFPE and PEI, the PFPE type (ester vs oxide), and the presence of potassium buffer on the hydrogels' linear and nonlinear viscoelasticity (Figures 3F–I). Hydrogels A–D manifest solid-like linear viscoelasticity (i.e., $G'(\omega) \gg G''(\omega)$, where $G''(\omega)$ exhibits a local minimum between 50 and 100 rad·s^{-1}, while $G'(\omega)$ is nearly frequency-independent within the investigated frequency range [Figures 3F and 3H]). The plateau value of the elastic modulus is on the order of 104 Pa regardless of the composition. Such behavior results from the assembly of F127 micelles into a colloidal gel[28,29] and is commonly observed in other gel systems.[30,31] The nonlinear rheology of our hydrogels was probed through large amplitude oscillatory shear (LAOS) experiments, where G' and G'' are plotted as functions of the strain amplitude γ_0. A linear viscoelastic domain (i.e., a region where G' and G'' are nearly independent of γ_0) is typically

observed for $\gamma_0 < 10-2$. At larger strain amplitudes, G' decreases while G'' marks an overshoot and eventually decreases as well. This nonlinear region is characterized by a crossover (a shift from $G' > G''$ to $G' < G''$), indicating a strain-induced fluidization of the hydrogels. The yield stress associated with this transition varies from 380 to 650 Pa depending on the hydrogels' composition (Figure 3F−I). Such LAOS behavior is a typical feature of many soft materials[32] and is believed to be caused by a rearrangement of the network structure during the yielding process.

Although some differences are observed between the tested hydrogel formulations, mostly in G'', the overall rheological behavior in both linear and nonlinear domains is very consistent (Figures 3F−H). Rheological behaviors of PFPE containing hydrogels (Hydrogels A−D) seem to be mostly controlled by the gel matrix of F127 and glycerol, with little influence from the incorporated PFPE and/or PEI (Supporting Information Figures S3−4). To investigate this, two control hydrogels were prepared, hydrogel E that lacks PFPE and an additional hydrogel control lacking both PEI and PFPE, representing an F127/glycerol matrix in water. The rheological behaviors of these gels were compared to hydrogels A and C. Data indicates that the presence of PEI does not change the native F127/glycerol matrix rheology (Figure S3) and that the presence of PFPE has a minimal impact on the overall rheological behavior of the F127/glycerol matrix (Figure S4). This is a critical finding, indicating that the presented hydrogels can be modified for a variety of applications in which PFPE and PEI are added for the purposes of imaging, or as therapeutic/diagnostic carriers, without causing a significant change in overall hydrogel performance. Further, it indicates that the presented hydrogels are robust thermoresponsive materials which can tolerate inclusion of highly hydrophobic dispersions (PFPE) and highly charged moieties (PEI).

As mentioned previously, the PFPE/PEI ionic bond may be influenced by changes in hydrogel pH. To further investigate this, the pH, rheology, and droplet surface area of PFPE ester hydrogels with and without potassium buffer were evaluated over time (Figure 4). Regardless of storage temperature, nonbuffered hydrogel pH rapidly decreases within 2 weeks of production, whereas buffered hydrogel pH remains constant for 25 days (Figure 4A). This pH decrease is likely caused by disruption of the PFPE/PEI ionic interaction, resulting in transformation of the free carboxylate ion to a carboxylic acid. This hydrolysis and subsequent emulsion droplet degradation were found to impact hydrogel rheological behavior. Hydrogel B (buffered) shows no change in rheological properties over 30 days of storage (Figure 4B). However, both the elastic and viscous moduli (G' and G'') are impacted by day 30 when the hydrogel is not buffered (Figure 4C).

Microscopic images of hydrogels B and A (with and without buffer) confirmed that emulsion droplets completely degrade within 90 days when the hydrogel is not buffered (Figures 4E−F). Buffered hydrogel B appears unchanged after 90 days of storage (Figures 4H−I). This visual observation was quantitatively confirmed using the same algorithm described earlier. Hydrogels A and B have similar droplet size and distribution when they are initially produced, but by day 90, nonbuffered hydrogel A contains few droplets that can be measured, while buffered hydrogel B droplet size is not significantly impacted (Figures 4D, 4G, Table 2). Therefore, inclusion of potassium buffer in the PFPE/PEI/F127 hydrogel is required to maintain its colloidal, pH, and rheological

Table 2. Median Droplet Surface Area of PFPE Ester Hydrogels with and without Potassium Buffer at Time t = 0 and t = 90 days after Production

	Time $t = 0$	Time $t = 90$ days
Hydrogel A (Without Buffer)	7.438 μm^2	17.768 μm^2
Hydrogel B (With Buffer)	7.264 μm^2	6.785 μm^2

stability. Buffer inclusion preserves the PFPE/PEI ionic interaction, preventing emulsion droplet degradation.

The ultimate use of the presented hydrogels is for drug and oxygen delivery supported by ^{19}F MRI. PFPE provides a strong ^{19}F MR signal without impacting hydrogel rheological behavior. Hence, the imaging agent is not expected to confound the delivery properties of the material, which is critical for its future biomedical use. We also evaluated in vitro MR properties of hydrogel A (Figure 5). The ^{19}F images are displayed in hot iron pseudo color and represent two consecutive slices through hydrogel samples (Figures 5A−B). Images and ^{19}F MR signal quantifications demonstrate concentration-dependent ^{19}F signal (Figure 5C). Therefore, we posit that these materials can be easily and quantitatively monitored in living subjects by ^{19}F MR upon implantation and throughout their use for drug and/or oxygen delivery.

To demonstrate the hydrogel's potential as a drug delivery platform, the natural anti-inflammatory compound resveratrol was incorporated into the developed hydrogel. To accomplish this, resveratrol-loaded F127 micelles (5 mg/mL resveratrol, 50 mg/mL F127) were prepared by adapting previously reported solvent casting methods.[33,34] Developed micelles were 22.05 ± 0.22 nm in diameter (Supporting Information Figure S5) and encapsulated resveratrol at a concentration of 4.66 ± 0.05 mg/mL resveratrol (93.24 ± 0.93% efficacy). This approach enabled the incorporation of a poorly water-soluble compound into the hydrogel without significantly altering hydrogel composition.

Three resveratrol-loaded hydrogels were developed and evaluated for drug loading (Table 3). Hydrogel F, a resveratrol-loaded version of Hydrogel A (Table 1), contained PEI-stabilized PFPE emulsion droplets, as confirmed by cross-polarized optical microscopy (Supporting Information Figure S6). A PFPE-free hydrogel with PEI (Hydrogel G) and a PEI/PFPE-free hydrogel (Hydrogel H) were developed as controls. Hydrogel resveratrol content was quantified using HPLC 48 h after production (Table 3, Figure 6A). Hydrogels F and H fully incorporated resveratrol, while Hydrogel G contained significantly less resveratrol, possibly due to an interaction between resveratrol and PEI, which is a highly charged, basic polymer. PEI cross-linking with PFPE (Hydrogel F) prevents this decrease in drug loading.

Hydrogels F and H were further evaluated for resveratrol release at ambient temperature using Slide-A-Lyzer dialysis cassettes (Figure 6B). Resveratrol micelle was used as a control. Hydrogels F and H demonstrate comparable release profiles, suggesting that the presence of PFPE-PEI emulsion droplets does not impact resveratrol release. The resveratrol micelle mimics saturation binding kinetics ($R^2 = 0.9987$), with a maximum release of 86% achieved at 271 h (approximately 11 days). Hydrogels F and H released resveratrol more slowly than the micelle control, with linear release extending to 291 h ($R^2 > 0.98$). This suggests that hydrogels could be used for extended drug delivery. It is imperative that these materials do not impair cellular viability or cause tissue damage.
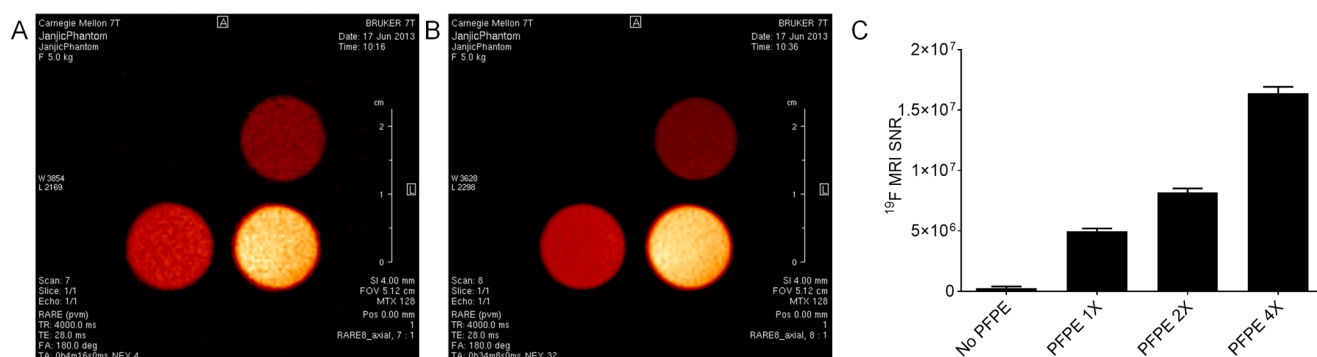
Figure 5. (A–B) ^{19}F MR images of two consecutive scans of the hydrogels with increasing concentration of dispersed PFPE droplets, displayed in hot iron pseudo color. (C) Higher hydrogel PFPE concentration corresponds to higher MRI signal-to-noise ratio.

Table 3. Composition and Drug Loading of Resveratrol Hydrogels

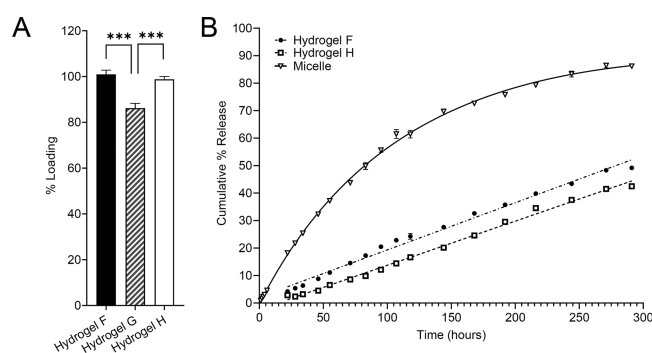|	Composition				Drug Loading	
Hydrogel	Pluronic F127 (% w/v)	Glycerol (% w/v)	PEI (25 kDa) (% w/v)	PFPE Ester (% w/v)	Resveratrol Concentration (μg/g gel)	% Loading
F	21.00	24.47	0.07	12.24	531 ± 10	101.0 ± 1.9
G	21.00	24.47	0.07		472 ± 11	86.2 ± 2.1
H	21.00	24.47			553 ± 7	98.8 ± 1.2

Figure 6. Drug loading and release profile of PFPE/PEI/F127 hydrogel (Hydrogel F) and controls. (A) Resveratrol (model drug) loading in hydrogel F compared to PFPE-free hydrogel containing PEI (Hydrogel G) and pure F127 hydrogel control (Hydrogel H). The presence of unconjugated PEI in PFPE-free hydrogel (Hydrogel G) significantly decreases resveratrol loading compared to cross-linked hydrogel F. (B) The presence of PFPE-PEI emulsion droplets does not significantly affect the resveratrol release profile as compared to pure F127 (Hydrogel H) while both gels show extended release.

Figure 7. Cell viability measured by RAW 264.7 cells exposure to increasing concentrations of Hydrogel A (PFPE-Ester/PEI/F127 cross-linked hydrogel) and Hydrogel E (control hydrogel prepared with PEI and F127 without added PFPE). Cells are cultured in complete medium for 24 h before cell viability is measured by luminescence following exposure to Cell Titer Glo assay reagents. Data represents the mean ± SD of triplicate measurements.

Though all the components in the developed hydrogel have been safely used in humans, PEI can be cytotoxic. The reducible disulfide linkages and ester conjugation have both been shown to minimize PEI toxicity.[35] Similarly, PFPE/PEI ionic interaction prevents PEI-induced cellular membrane destabilization. To verify the safety of the developed hydrogel, PFPE-Ester/PEI hydrogel (Hydrogel A) was evaluated for toxicity in a murine macrophage cell line. As a control, a PFPE-free version of the hydrogel was also evaluated (Hydrogel E). Figure 7 shows that hydrogel A is nontoxic at concentrations of up to 50 mg/mL, whereas Hydrogel E demonstrates dose-dependent toxicity at concentrations of greater than 6.25 mg/mL.

In conclusion, we present here a novel PFPE-loaded thermoresponsive hydrogel designed for ^{19}F MR supported delivery. Our results show that PFPE can be successfully incorporated into a hydrogel by using planetary mixing while the surf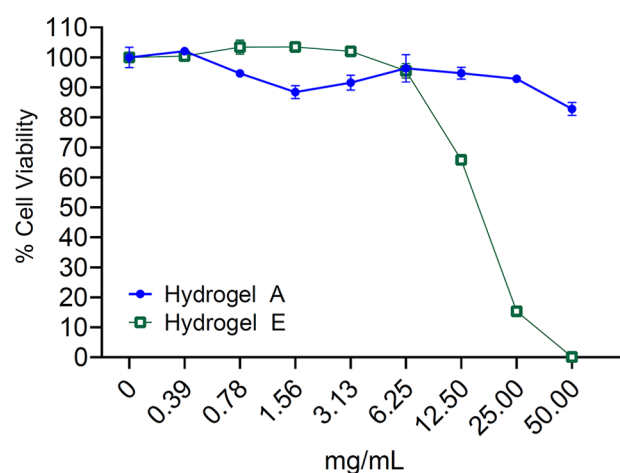aces of distributed PFPE droplets are cross-linked with branched PEI. The low-energy planetary mixing used to cross-link PEI and PFPE ester can be used to incorporate a wide variety of payloads into the hydrogel, including fluorescent dyes, pH sensors, chelators, drugs, and antibodies. The data indicates that the presented hydrogels are robust thermoresponsive materials that tolerate the inclusion of highly hydrophobic dispersions (PFPE) and highly charged moieties (PEI) without impacting the F127-driven rheological properties of the hydrogel. The presence of PFPE and PEI in the hydrogels gives rise to a high level of functionalization opportunities, which renders this new biomaterial highly versatile and easy to produce, facilitating future scale-up and good manufacturing practice (GMP) production.

■ ASSOCIATED CONTENT

Supporting Information

The Supporting Information is available free of charge at https://pubs.acs.org/doi/10.1021/acsmedchemlett.0c00198.

Materials, experimental procedures and methods, and additional supplementary figures (PDF)

■ AUTHOR INFORMATION

Corresponding Author

Jelena M. Janjic − *Graduate School of Pharmaceutical Sciences, School of Pharmacy, Duquesne University, Pittsburgh, Pennsylvania 15282, United States;* orcid.org/0000-0002-0539-8359; Phone: 412-396-6369; Email: janjicj@duq.edu

Authors

Michele Herneisey − *Graduate School of Pharmaceutical Sciences, School of Pharmacy, Duquesne University, Pittsburgh, Pennsylvania 15282, United States*

Paula Flórez Salcedo − *Graduate School of Pharmaceutical Sciences, School of Pharmacy, Duquesne University, Pittsburgh, Pennsylvania 15282, United States*

Trystan Domenech − *Swanson School of Engineering, University of Pittsburgh, Pittsburgh, Pennsylvania 15260, United States*

Christina Bagia − *Graduate School of Pharmaceutical Sciences, School of Pharmacy, Duquesne University, Pittsburgh, Pennsylvania 15282, United States*

Simon S. George − *Graduate School of Pharmaceutical Sciences, School of Pharmacy, Duquesne University, Pittsburgh, Pennsylvania 15282, United States*

Robert Tunney − *Graduate School of Pharmaceutical Sciences, School of Pharmacy, Duquesne University, Pittsburgh, Pennsylvania 15282, United States*

Sachin Velankar − *Swanson School of Engineering, University of Pittsburgh, Pittsburgh, Pennsylvania 15260, United States*

T. Kevin Hitchens − *Department of Neurobiology, University of Pittsburgh, Pittsburgh, Pennsylvania 15260, United States*

Complete contact information is available at:
https://pubs.acs.org/10.1021/acsmedchemlett.0c00198

Author Contributions

||The manuscript was written through contributions of all authors. M.H. and P.F. contributed to the paper equally and serve as cofirst authors. T.D. performed rheological studies and collected and analyzed data. T.K.H. performed MRI and analyzed data. S.V. codesigned the analytical portion of the study with J.M.J., interpreted the rheological results, and guided rheology studies. C.B., R.T., and S.G. manufactured hydrogels per J.M.J. input and collected data for quality control including size measurements, imaging, and pH studies. J.M.J. designed the PFPE/PEI/F127 hydrogels and manufacturing and assessment protocols, designed and led the study, cowrote the manuscript, analyzed data, and constructed key figures.

Notes

The authors declare no competing financial interest.

■ ACKNOWLEDGMENTS

■ ABBREVIATIONS

PFC, perfluorocarbon; PFPE, perfluoropolyether; MRI, magnetic resonance imaging; PEI, polyethylenimine; LAOS, large amplitude oscillatory shear

■ REFERENCES

(1) Krafft, M. P. Fluorocarbons and fluorinated amphiphiles in drug delivery and biomedical research. *Adv. Drug Delivery Rev.* **2001**, *47* (2−3), 209−228.

(2) Ahrens, E. T.; Flores, R.; Xu, H.; Morel, P. A. In vivo imaging platform for tracking immunotherapeutic cells. *Nat. Biotechnol.* **2005**, *23* (8), 983−7.

(3) Hertlein, T.; Sturm, V.; Jakob, P.; Ohlsen, K. [19]F magnetic resonance imaging of perfluorocarbons for the evaluation of response to antibiotic therapy in a Staphylococcus aureus infection model. *PLoS One* **2013**, *8* (5), No. e64440.

(4) Temme, S.; Bonner, F.; Schrader, J.; Flogel, U. [19]F magnetic resonance imaging of endogenous macrophages in inflammation. *Wiley Interdiscip Rev. Nanomed Nanobiotechnol* **2012**, *4* (3), 329−43.

(5) Tonelli, C.; Gavezotti, P.; Strepparola, E. Linear perfluoropolyether difunctional oligomers: chemistry, properties and applications. *J. Fluorine Chem.* **1999**, *95* (1−2), 51−70.

(6) Janjic, J. M.; Srinivas, M.; Kadayakkara, D. K. K.; Ahrens, E. T. Self-delivering Nanoemulsions for Dual Fluorine-19 MRI and Fluorescence Detection. *J. Am. Chem. Soc.* **2008**, *130* (9), 2832−2841.

(7) Patrick, M. J.; Janjic, J. M.; Teng, H.; O'Hear, M. R.; Brown, C. W.; Stokum, J. A.; Schmidt, B. F.; Ahrens, E. T.; Waggoner, A. S. Intracellular pH measurements using perfluorocarbon nanoemulsions. *J. Am. Chem. Soc.* **2013**, *135* (49), 18445−57.

(8) Lowe, K. C.; Davey, M. R.; Power, J. B. Perfluorochemicals: their applications and benefits to cell culture. *Trends Biotechnol.* **1998**, *16* (6), 272−277.

(9) Ahmed, E. M. Hydrogel: Preparation, characterization, and applications: A review. *Journal of Advanced Research* **2015**, *6* (2), 105−121.

(10) Hoare, T. R.; Kohane, D. S. Hydrogels in drug delivery: Progress and challenges. *Polymer* **2008**, *49* (8), 1993−2007.

(11) Zheng Shu, X.; Liu, Y.; Palumbo, F. S.; Luo, Y.; Prestwich, G. D. In situ crosslinkable hyaluronan hydrogels for tissue engineering. *Biomaterials* **2004**, *25* (7−8), 1339−1348.

(12) Peppas, N. A.; Van Blarcom, D. S. Hydrogel-based biosensors and sensing devices for drug delivery. *J. Controlled Release* **2016**, *240*, 142−150.

(13) Lee, P. I.; Kim, C.-J. Probing the mechanisms of drug release from hydrogels. *J. Controlled Release* **1991**, *16* (1), 229−236.

(14) Bulte, J. W. M.; Modo, M. M. J. *Design and Applications of Nanoparticles in Biomedical Imaging*; Springer International Publishing: 2016.

(15) Wijekoon, A.; Fountas-Davis, N.; Leipzig, N. D. Fluorinated methacrylamide chitosan hydrogel systems as adaptable oxygen carriers for wound healing. *Acta Biomater.* **2013**, *9* (3), 5653−5664.

(16) Patil, P. S.; Fountas-Davis, N.; Huang, H.; Michelle Evancho-Chapman, M.; Fulton, J. A.; Shriver, L. P.; Leipzig, N. D. Fluorinated methacrylamide chitosan hydrogels enhance collagen synthesis in wound healing through increased oxygen availability. *Acta Biomater.* **2016**, *36*, 164−74.

(17) Akula, S.; Brosch, I. K.; Leipzig, N. D. Fluorinated Methacrylamide Chitosan Hydrogels Enhance Cellular Wound Healing Processes. *Ann. Biomed. Eng.* **2017**, *45* (11), 2693−2702.

(18) Patil, P. S.; Fathollahipour, S.; Inmann, A.; Pant, A.; Amini, R.; Shriver, L. P.; Leipzig, N. D. Fluorinated Methacrylamide Chitosan Hydrogel Dressings Improve Regenerated Wound Tissue Quality in

Diabetic Wound Healing. *Adv. Wound Care (New Rochelle)* **2019**, *8* (8), 374−385.

(19) Ma, T.; Zhu, L.; Yang, Y.; Quan, X.; Huang, L.; Liu, Z.; Sun, Z.; Zhu, S.; Huang, J.; Luo, Z. Enhanced in vivo survival of Schwann cells by a synthetic oxygen carrier promotes sciatic nerve regeneration and functional recovery. *J. Tissue Eng. Regener. Med.* **2018**, *12* (1), e177−e189.

(20) Chin, K.; Khattak, S. F.; Bhatia, S. R.; Roberts, S. C. Hydrogel-perfluorocarbon composite scaffold promotes oxygen transport to immobilized cells. *Biotechnol. Prog.* **2008**, *24* (2), 358−66.

(21) White, J. C.; Stoppel, W. L.; Roberts, S. C.; Bhatia, S. R. Addition of perfluorocarbons to alginate hydrogels significantly impacts molecular transport and fracture stress. *J. Biomed. Mater. Res., Part A* **2013**, *101* (2), 438−46.

(22) Liu, L.; Bagia, C.; Janjic, J. M. The First Scale-Up Production of Theranostic Nanoemulsions. *BioRes. Open Access* **2015**, *4* (1), 218−28.

(23) Gioffredi, E.; Boffito, M.; Calzone, S.; Giannitelli, S. M.; Rainer, A.; Trombetta, M.; Mozetic, P.; Chiono, V. Pluronic F127 Hydrogel Characterization and Biofabrication in Cellularized Constructs for Tissue Engineering Applications. *Procedia CIRP* **2016**, *49*, 125−132.

(24) Kavand, A.; Anton, N.; Vandamme, T.; Serra, C. A.; Chan-Seng, D. Synthesis and functionalization of hyperbranched polymers for targeted drug delivery. *J. Controlled Release* **2020**, *321*, 285−311.

(25) Badawi, A. A.; El-Nabarawi, M. A.; El-Setouhy, D. A.; Alsammit, S. A. Characterization and stability testing of itraconazole solid dispersions containing crystallization inhibitors. *Am. J. Drug Discovery Dev.* **2011**, *1*, 144

(26) Persico, D. F.; Gerhardt, G. E.; Lagow, R. J. Synthesis of perfluoropolyethers via hydrocarbon polyesters: a new general method. *J. Am. Chem. Soc.* **1985**, *107* (5), 1197−1201.

(27) Patil, P. S.; Leipzig, N. D. Fluorinated Methacrylamide Chitosan Sequesters Reactive Oxygen Species to Relieve Oxidative Stress while Delivering Oxygen. *J. Biomed. Mater. Res., Part A* **2017**, *105* (8), 2368−2374.

(28) Bromberg, L. E.; Ron, E. S. Temperature-responsive gels and thermogelling polymer matrices for protein and peptide delivery. *Adv. Drug Delivery Rev.* **1998**, *31* (3), 197−221.

(29) Jiang, J.; Li, C.; Lombardi, J.; Colby, R. H.; Rigas, B.; Rafailovich, M. H.; Sokolov, J. C. The effect of physiologically relevant additives on the rheological properties of concentrated Pluronic copolymer gels. *Polymer* **2008**, *49* (16), 3561−3567.

(30) Erwin, B. M.; Cloitre, M.; Gauthier, M.; Vlassopoulos, D. Dynamics and rheology of colloidal star polymers. *Soft Matter* **2010**, *6* (12), 2825−2833.

(31) Koumakis, N.; Petekidis, G. Two step yielding in attractive colloids: transition from gels to attractive glasses. *Soft Matter* **2011**, *7* (6), 2456−2470.

(32) Hyun, K.; Wilhelm, M.; Klein, C. O.; Cho, K. S.; Nam, J. G.; Ahn, K. H.; Lee, S. J.; Ewoldt, R. H.; McKinley, G. H. A review of nonlinear oscillatory shear tests: Analysis and application of large amplitude oscillatory shear (LAOS). *Prog. Polym. Sci.* **2011**, *36* (12), 1697−1753.

(33) Rao, D. A.; Cote, B.; Stammet, M.; Fatease, A. M. A.; Alani, A. W. Evaluation of the Stability of Resveratrol Pluronic Micelles Prepared by Solvent Casting and Simple Equilibrium Methods. *Pharm. Nanotechnol.* **2016**, *4*, 120−125.

(34) Carlson, L. J.; Cote, B.; Alani, A. W.; Rao, D. A. Polymeric micellar co-delivery of resveratrol and curcumin to mitigate in vitro doxorubicin-induced cardiotoxicity. *J. Pharm. Sci.* **2014**, *103* (8), 2315−22.

(35) Zhang, X.-Z.; Zeng, X.; Sun, Y.-X.; Zhuo, R.-X. Bioactive materials in gene therapy. In *Bioactive Materials in Medicine*; Zhao, X., Courtney, J. M., Qian, H., Eds.; Woodhead Publishing: 2011; pp 179−219.